Water Uptake and Distribution in Germinating Tobacco Seeds Investigated in Vivo by Nuclear Magnetic Resonance Imaging[1][w]

Bertram Manz, Kerstin Müller, Birgit Kucera, Frank Volke, and Gerhard Leubner-Metzger*

Fraunhofer-Institut für Biomedizinische Technik, Arbeitsgruppe Magnetische Resonanz, D–66386 St. Ingbert, Germany (B.M., F.V.); and Institut für Biologie II, Botanik/Pflanzenphysiologie, Albert-Ludwigs-Universität Freiburg, D–79104 Freiburg i. Br., Germany (K.M., B.K., G.L.-M.)

The regulation of water uptake of germinating tobacco (*Nicotiana tabacum*) seeds was studied spatially and temporally by in vivo ^{1}H-nuclear magnetic resonance (NMR) microimaging and ^{1}H-magic angle spinning NMR spectroscopy. These nondestructive state-of-the-art methods showed that water distribution in the water uptake phases II and III is inhomogeneous. The micropylar seed end is the major entry point of water. The micropylar endosperm and the radicle show the highest hydration. Germination of tobacco follows a distinct pattern of events: rupture of the testa is followed by rupture of the endosperm. Abscisic acid (ABA) specifically inhibits endosperm rupture and phase III water uptake, but does not alter the spatial and temporal pattern of phase I and II water uptake. Testa rupture was associated with an increase in water uptake due to initial embryo elongation, which was not inhibited by ABA. Overexpression of β-1,3-glucanase in the seed-covering layers of transgenic tobacco seeds did not alter the moisture sorption isotherms or the spatial pattern of water uptake during imbibition, but partially reverted the ABA inhibition of phase III water uptake and of endosperm rupture. In vivo ^{13}C-magic angle spinning NMR spectroscopy showed that seed oil mobilization is not inhibited by ABA. ABA therefore does not inhibit germination by preventing oil mobilization or by decreasing the water-holding capacity of the micropylar endosperm and the radicle. Our results support the proposal that different seed tissues and organs hydrate at different extents and that the micropylar endosperm region of tobacco acts as a water reservoir for the embryo.

Water uptake is the fundamental requirement for the initiation and completion of seed germination. Water, oxygen, and an appropriate temperature are necessary and sufficient for a mature, nondormant seed to complete germination. The completion of germination is manifested as radicle protrusion, i.e. the emergence of the radicle tip through all seed-covering layers. It depends on embryo expansion, which is a process driven by water uptake and cell wall loosening (Bewley, 1997b; Obroucheva and Antipova, 1997; Koornneef et al., 2002). Uptake of water by a dry seed is triphasic with a rapid initial uptake (phase I, i.e. imbibition) followed by a plateau phase (phase II). A further increase in water uptake occurs only after germination is completed, as the embryo axes elongate. Because dormant seeds do not complete germination, they do not enter this postgermination phase of water uptake (phase III). Abscisic acid (ABA) inhibits phase III water uptake and the transition from germination to postgermination growth (e.g. Schopfer and Plachy, 1984; Leubner-Metzger et al., 1995). In Arabidopsis (*Arabidopsis thaliana*) the transcription factor ABI5 is known to be required for the developmental switch from germination to postgermination growth (Finkelstein and Lynch, 2000; Lopez-Molina et al., 2001). While the temporal pattern of water uptake by seeds has been well studied in different species, only very little is known about its spatial pattern and how it is affected by the inhibitory effect of ABA on seed germination.

Tobacco (*Nicotiana tabacum*) is an established model system for the germination of endospermic seeds (Koornneef et al., 2002; Leubner-Metzger, 2003). The embryo in mature tobacco seed is surrounded by three to five layers of endosperm cells and a thin testa (seed coat), which consists of an outer layer of cutinized and lignified dead cells and a living inner testa layer. Both covering layers, the testa and the endosperm, are a hindrance to seed germination of tobacco and other Solanaceae. Testa rupture and endosperm rupture, which always occur at the micropylar seed end, are distinct and temporally separate events during the germination of tobacco. This experimental advantage was used to study the hormonal regulation and to pinpoint the sites for class I β-1,3-glucanase (βGlu I) action (e.g. Leubner-Metzger and Meins, 2000; Leubner-Metzger, 2002, 2005). ABA inhibits the induction of βGlu I in the micropylar endosperm just before its rupture but does not affect testa rupture of tobacco. ABA also inhibits endosperm rupture, but not testa rupture, of several other Nicotiana species and of

[1] This work was supported by the Wissenschaftliche Gesellschaft Freiburg (grant to G.L.-M.) and the Deutsche Forschungsgemeinschaft (grant no. DFG LE 720/3 to G.L.-M.).

* Corresponding author; e-mail gerhard.leubner@biologie.uni-freiburg.de; fax 49–761–203–2612.

[w] The online version of this article contains Web-only data.

Article, publication date, and citation information can be found at www.plantphysiol.org/cgi/doi/10.1104/pp.105.061663.

petunia (*Petunia hybrida*; Grappin et al., 2000; Krock et al., 2002; Petruzzelli et al., 2003; Schwachtje and Baldwin, 2004). Transgenic TKSG7 tobacco seeds overexpress βGlu I in the seed-covering layers under the control of a chimeric ABA-inducible transgene promoter (Leubner-Metzger, 2003). The seed phenotype of TKSG7 differs from wild-type and TCIB1 (empty-vector, wild-type phenotype) in several aspects, including the finding that the βGlu I overexpression partially reverts the inhibitory effect of ABA on endosperm rupture. How this affects the temporal and spatial seed properties during water uptake has not been investigated.

^{1}H-NMR imaging (MRI) is a noninvasive in vivo technique that allows the acquisition of sequential cross-sectional two-dimensional (2D) and three-dimensional (3D) images of the spatial distribution of ^{1}H nuclei (protons; Mansfield and Morris, 1982; Callaghan, 1991; MacFall and van As, 1996; Ratcliffe, 1996; Fountain et al., 1998; Manz et al., 1999, 2003; Kamenetsky et al., 2003; Schneider et al., 2003). MRI relies on the principle that ^{1}H nuclei carry a nonzero spin and therefore a magnetic moment. NMR signals occur if these nuclei are immersed in a strong, static magnetic field and are exposed to energy delivered by a radio frequency pulse. The interaction of the magnetic moment with externally applied magnetic field gradients and radio frequencies is used to obtain 2D or 3D images. In cases where the resolved volume elements are finer than the resolution of the unaided human eye (approx. 0.1 mm), this method of imaging may be termed microscopic (Callaghan, 1991). MRI and ^{1}H-NMR microimaging (MRM) have been used to study water uptake and flow in relatively large seeds of legumes (Pouliquen et al., 1997; Fountain et al., 1998), trees (Carrier et al., 1999; Roh et al., 2004; Terskikh et al., 2005), and of cereal grains (Jenner et al., 1988; Chudek and Hunter, 1997; Hou et al., 1997; Gruwel et al., 2002; Köckenberger et al., 2004; Krishnan et al., 2004). Redistribution of water and tissue-specific differences in moisture content were detected in these seeds. Imbibition and germination of seeds as small as tobacco, i.e. <1 mm, has not been studied by NMR microimaging.

Spatially nonresolved NMR spectroscopy is a fast and accurate method for the determination of moisture content in biological samples (Schmidt, 1991). Over recent years, cheap mobile, low-field NMR instruments (Eidmann et al., 1996; Prado, 2001; Wolter, 2001) have been introduced, which enable the determination of oil/water content using a relaxation time analysis (LaTorraca et al., 1998; Korb et al., 2003). However, some results of water content reported in the literature turned out to be wrong, because hydrogen nuclei of molecules in the seed possess the same mobility as water with a kind of restricted motion (Volke et al., 1996). Therefore, a spectral-resolution enhancement using magic angle spinning (MAS)-^{1}H-NMR and -^{13}C NMR spectroscopy, which have only recently emerged as useful tools in plant biology (Bardet et al., 2001; Bardet and Foray, 2003; Schneider et al., 2003), yields much more accurate results. During MAS NMR spectroscopy the intact seeds are rotated at high speed around an axis inclined by 54.7° in relation to the magnetic field, which results in higher spectral resolution and sharper signals (peaks). The detected signals at specific frequencies can be used to identify specific substances. The peak intensities are correlated with the amount of spins contributing to a specific peak. Thus, qualitative and quantitative information about chemical bonds, molecular conformations and structures, and dynamic processes can be deduced by this nondestructive in vivo technique. MAS-^{13}C NMR spectroscopy has been used to identify triacyl glycerols (TAGs) in lettuce seeds (*Lactuca sativa*; Bardet et al., 2001; Bardet and Foray, 2003).

The work presented in this research paper demonstrates that these in vivo NMR methods are powerful tools for analyzing water uptake and distribution in seeds and for seed oil mobilization. They can be used to nondestructively explore the effect of the plant hormones and transgenes in seeds as small as tobacco. NMR microimaging showed that the micropylar region of the endosperm is a major entry point for water uptake during tobacco seed germination. Our results support the proposal that different seed tissues and organs hydrate at different extents and that the endosperm of tobacco acts as a water reservoir for the embryo. ABA and overexpression of βGlu I in transgenic tobacco seeds do not alter the spatial pattern of water uptake, but affect the temporal pattern and the transition to phase III water uptake. MAS-^{13}C NMR spectroscopy showed that ABA did not inhibit tobacco seed oil mobilization.

RESULTS

Spatial and Temporal Analyses by Nondestructive in Vivo ^{1}H-NMR Techniques of Water Uptake and Distribution during Tobacco Seed Germination

The water uptake during tobacco seed imbibition and germination was investigated nondestructively in vivo using ^{1}H-MAS NMR spectroscopy (Fig. 1). The water signal is evident at 4.8 ppm in the ^{1}H-MAS NMR spectra and the area of this water peak is a measure for the seed water content (Fig. 1A). Both the new nondestructive ^{1}H-MAS NMR spectroscopic method and the classical destructive gravimetric method showed that the temporal pattern of water uptake is triphasic (Fig. 2). The comparison of the two methods demonstrates that ^{1}H-MAS NMR spectroscopy is a powerful in vivo method to nondestructively investigate seed water contents. Testa rupture and endosperm rupture (i.e. radicle protrusion) are distinct and temporally separate events during the germination of tobacco (Leubner-Metzger, 2003). We utilized this experimental advantage of the tobacco seed model system to relate the distinct phases of water uptake and the effect

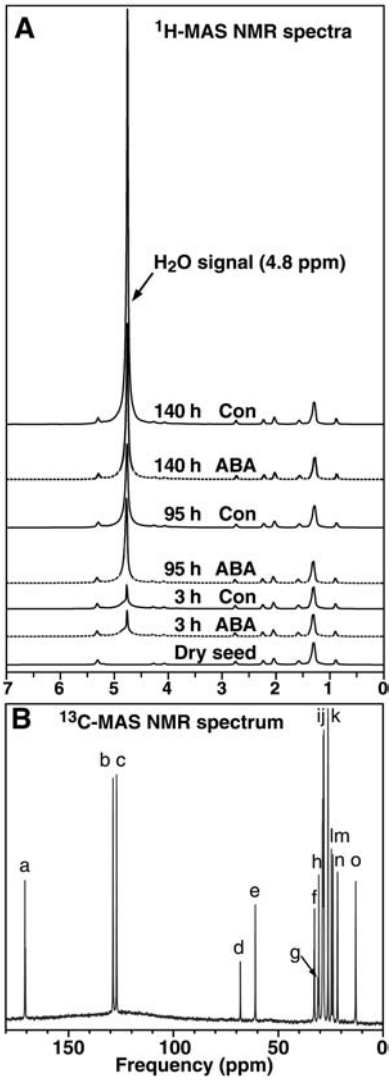

Figure 1. Representative in vivo ^{1}H-MAS NMR (A) and ^{13}C-MAS NMR (B) spectra of tobacco seeds. A, The area below the H_2O signal at 4.8 ppm was used to calculate the relative water uptake of tobacco seeds with time after the start of imbibition in medium without (Con) and with (ABA) 10 μM ABA, which is presented in Figure 2B. B, The assignment of glycerol and fatty acid peaks according to Bardet et al. (2001). Glycerol (d and e), C18:1Δ9 + C18:2 (a, b, i, j, and m–o), C18:2 (c, h, and l), C18:1Δ9 (f and g). The relative contents per seed presented in Figure 2C were calculated from the corresponding peak heights.

of ABA on water uptake to these visible markers of the germination process (Fig. 2, A and B).

The temporal pattern of phases I and II of water uptake were identical for seeds imbibed in medium without (control) and with 10 μM ABA (Figs. 1 and 2). Phase I (imbibition) of water uptake was completed within a few hours, and after 1 d a typical phase II plateau with a seed water content of 40 to 50 μg water/seed, i.e. approximately 40% water per fresh weight (FW), was obtained (Fig. 2B). Testa rupture is not inhibited by ABA and is associated with an additional increase in seed water content to 60 to 70 μg water/seed, i.e. approximately 50% water per FW. This additional increase in the seed water content, which occurs at the end of phase II, was evident in the control and ABA series, and was associated with the process of testa rupture and initial embryo elongation. Phase III water uptake occurred only in the control (Figs. 1 and 2) and was associated with endosperm rupture and embryo growth. ABA inhibited phase III water uptake and endosperm rupture.

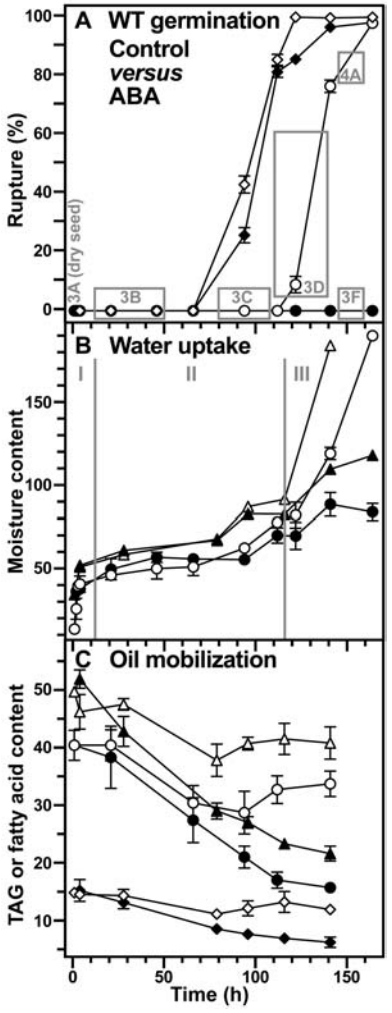

Figure 2. Time course analyses of water uptake and oil mobilization during wild-type tobacco seed germination. A, The incidence of testa rupture (◇, ♦) and endosperm rupture (○, ●) expressed as percent of approximately 100 seeds scored with time after the start of imbibition in medium without (Control, white symbols) and with (ABA, black symbols) 10 μM ABA. The gray boxes and their numbers correspond to the sections of Figures 3 and 4 showing in vivo NMR microimaging of seeds from these time windows. B, Water uptake measured gravimetrically (○, ●; micrograms water per seed) and by in vivo ^{1}H-MAS NMR (△, ▲; relative values per seed); Control (white symbols), ABA (black symbols). I, II, and III are the three phases of water uptake as described in the text. C, Seed oil mobilization measured biochemically as triacylglycerides (TAG, ○, ●; micrograms per seed) and by in vivo ^{13}C-MAS NMR (linoleic acid, △, ▲; oleic acid, ◇, ♦; relative contents per seed); Control (white symbols), ABA (black symbols). Mean ± SE of at least three samples are presented for each time point. When error bars are not shown, the ±SE values are <2 (A) or <1 (B and C).

NMR microimaging was used to measure the spatial distribution of protons in tobacco seeds (Fig. 3). In dry seeds (Fig. 3A) the proton signal strength is given by the content of water plus lipids in the sample (Schneider et al., 2003; Leubner-Metzger, 2005). The water signal at 4.8 ppm in the ^{1}H-MAS NMR spectra was the only signal that increased during water uptake (Fig. 1A). It is the major signal in phase II and III seeds. The proton signal is therefore essentially a water signal in these phases. Figures 3 and 4 show the water distribution of tobacco seeds and seedlings. Each section corresponds to a time window presented in Figure 2A as a gray box. Each of the sections (Fig. 3, B–E) shows ^{1}H-NMR 2D slices, which were taken from the full 3D microimages as serial sections through three single seeds (one per row) at the given stage. Longitudinal sections are presented in the first two rows (corresponding to Fig. 3I) and transverse sections are presented in the third row (corresponding to Fig. 3H) of each section. The enlarged ^{1}H-NMR 2D slices in the testa rupture stage (Fig. 3F) and the endosperm rupture stage (Fig. 3G) are selected images from Figure 3, C and D, respectively. For comparison, microphotographs of seeds in the corresponding stages are presented at the left sides of Figure 3, F and G. These ^{1}H-NMR microimages demonstrate that this method can be used to nondestructively analyze water distribution in seeds as small as tobacco, that is $<$1 mm.

The water distribution in phase II and III tobacco seeds in control medium was inhomogeneous (Fig. 3). The micropylar endosperm and the radicle were the tissues with the highest water content. These tissues have a significantly higher water content compared to the nonmicropylar endosperm and the cotyledons. This was already evident before testa rupture (Fig. 3B) and was even more pronounced after testa rupture (Fig. 3, C and F) and after endosperm rupture (Fig. 3, D and G). The thin outer testa (Fig. 3, H and I) is a dead and lignified tissue layer with which no appreciable hydration appears to be associated (Fig. 3, B–G). This is consistent with the finding that the tobacco seed has no appreciable mucilage layer (Avery, 1933). Also immediately after endosperm rupture the emerged radicle tip (arrows in Fig. 3D) and the micropylar endosperm are the tissues with the highest water contents (Fig. 3, D and G).

Figure 4 shows ^{1}H-NMR microimages of the water distribution in germinated tobacco seedlings (radicle emerged) at 150 h, i.e. before cotyledon emergence. The hypocotyl, the remainder of the endosperm, and the cortex of the root are the tissues with the highest water content. Within the root, the stele (yellow) is surrounded by a ring-shaped area of lower water content (red) that is likely to include the endodermis/pericycle region. This ring-shaped area is surrounded by cortex tissue with higher water content (yellow). Within the hypocotyl, the cortex appears to be the tissue with the highest water content. The cotyledons show a more or less homogenous medium-level water content.

Figure 3E shows ^{1}H-NMR microimages of the water distribution in ABA-imbibed tobacco seeds at 150 h, i.e. after testa rupture but before endosperm rupture. The water distribution in these ABA-treated seeds was like in the phase II control seeds before endosperm rupture (Fig. 3C). The micropylar endosperm and the radicle of ABA-treated wild-type seeds were the tissues with highest water content (Fig. 3E). Thus, although ABA inhibits phase III water uptake and endosperm rupture, it does not alter the spatial water distribution. ABA therefore does not inhibit germination by preventing the water-holding capacity of the micropylar endosperm and the radicle.

Nondestructive in Vivo ^{13}C-MAS NMR Spectroscopy Shows That ABA Does Not Inhibit Tobacco Seed Oil Mobilization

Tobacco seeds are oilseeds and dry seeds of the Havana-425 cultivar contain approximately 43% TAGs; seed oil) per FW, i.e. approximately 41 μg per seed (Fig. 2C). Similar TAG contents were obtained for other tobacco varieties (Frega et al., 1991). Although oil mobilization is mainly a postgermination event, it starts already prior to testa rupture. The TAG content decreased from approximately 41 to approximately 32 μg per seed prior to testa rupture and remained constant during testa and endosperm rupture of tobacco seeds imbibed in control medium (Fig. 2C). Interestingly, in ABA-imbibed seeds, there is a further decline to 16 μg per seed (Fig. 2C).

^{13}C-MAS NMR spectroscopy was used as nondestructive in vivo method to further investigate TAG mobilization during and after tobacco seed germination (Fig. 2C). The major fatty acids in tobacco seed TAGs are linoleic acid (C18:2; 60%–80%), oleic acid (C18:1Δ9; 10%–20%), and palmitic acid (C16:0; 10%–20%; Bush and Grunwald, 1972; Frega et al., 1991). In agreement with this, we detected approximately 3-fold higher levels of C18:2 in dry Havana-425 seeds, compared to C18:1Δ9 and C16:0 (Fig. 1B). The C18:2, C18:1Δ9 (Fig. 2C), and C16:0 (data not shown) contents measured by ^{13}C-MAS NMR spectroscopy exhibited the same temporal pattern as the TAG contents measured by the classical destructive method. They remained constant during testa and endosperm rupture in the control, but declined in ABA-imbibed seeds (Fig. 2C). Thus, ABA does not inhibit endosperm rupture of tobacco via the inhibition of seed oil mobilization.

βGlu I Overexpression in the Seed-Covering Layers Partially Reverts the ABA Inhibition of Phase III Water Uptake and of Endosperm Rupture

Since βGlu I overexpression in the covering layers replaces seed after-ripening in the low-hydrated stage and partially reverts the ABA inhibition of endosperm rupture in the fully imbibed seed stage (Leubner-Metzger, 2003, 2005), we wanted to know whether

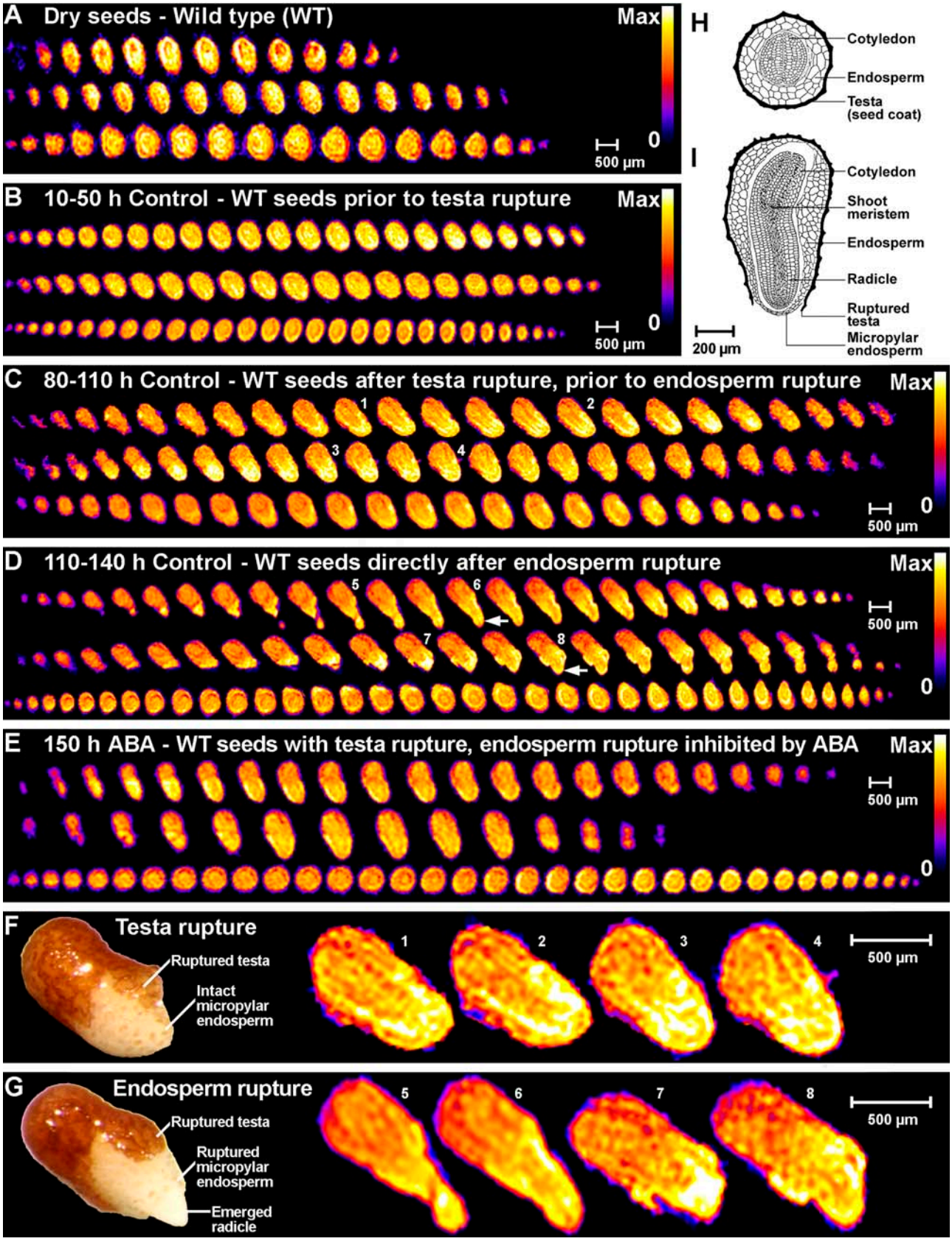

Figure 3. Noninvasive in vivo MRM analyses of water uptake and distribution during wild-type tobacco seed germination. The spatial distribution of protons within the seed tissues is visualized by false colors (relative scales from zero [0, black] to maximum

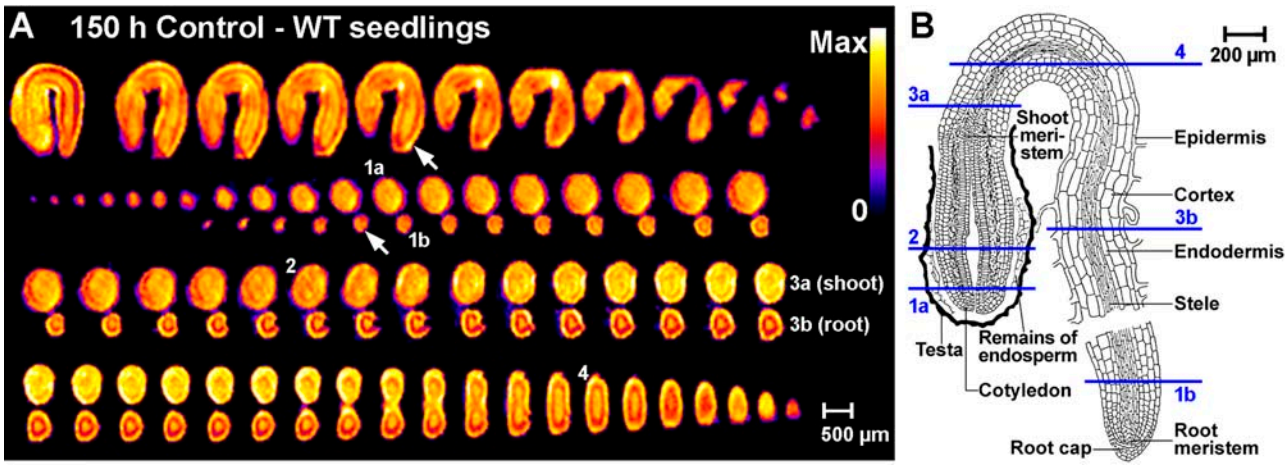

Figure 4. Noninvasive in vivo MRM analyses of germinated wild-type tobacco seedlings. The proton signal is indicative for the water signal; details as in Figure 3. A, Water distribution in germinated seedlings. Top row, NMR microimages as longitudinal serial sections. Bottom three rows, Transverse serial microimages through one seedling. Small white arrows indicate the emerged root tip. B, Drawing of a germinated tobacco seedling is from Avery (1933). Note that the numbers in A indicate corresponding transverse sections shown in the drawing in B.

these transgenic seeds are altered with regard to their water behavior. We therefore compared water uptake of TKSG7 (βGlu I overexpressing) and TCIB1 (empty-vector control, wild-type phenotype with regard to βGlu I and germination) tobacco seeds. Figure 5 shows moisture sorption isotherms of TKSG7 and TCIB1 tobacco seeds. These were obtained by incubating the seeds for 2 weeks at defined relative air humidities, which caused specific equilibrium seed moisture contents. Wild-type (data not shown) and TCIB1 (Fig. 5) tobacco seeds exhibited a typical oilseed moisture sorption isotherm. The transition from region 1 to 2 was at approximately 20% relative air humidity and was associated with approximately 7% overall seed moisture content. The transition from region 2 to 3 was at approximately 80% relative air humidity and was associated with approximately 12% overall seed moisture content. There was no difference in the moisture sorption isotherm curves between TKSG7 and TCIB1 and between freshly harvested and after-ripened seeds (Fig. 5). Thus, βGlu I overexpression and after-ripening did not affect the overall water-holding capacity of tobacco seeds incubated in humid air at room temperature.

In contrast to the situation in humid air, the temporal pattern of phase III water uptake during seed imbibition in ABA-containing medium was altered by βGlu I overexpression in the covering layers (Fig. 6). The inhibition by ABA of endosperm rupture and of phase III water uptake was partially reverted in the TKSG7 seeds compared to TCIB1 seeds. These differences were equally detectable by the ^{1}H-MAS NMR spectroscopic method and the gravimetric method (Fig. 6B).

Figure 7 shows ^{1}H-NMR microimages of the water distribution in ABA-imbibed TKSG7 and TCIB1 seeds after 110 h corresponding to the time windows presented in Figure 6A as gray boxes. Additional ^{1}H-NMR microimages of the water distribution in ABA-imbibed TKSG7 and TCIB1 seeds of earlier time points are presented in Supplemental Figure 1. Spatial water distribution in phase II water uptake stages did

Figure 3. (*Continued.*)
signal strength [max, white]). A scale bar is given as a size marker. The NMR microimages were obtained with approximately 30 μm resolution. A, Serial sections through three dry seeds, the proton signal is indicative for the water plus lipid signal. B to E, The proton signal during imbibition and germination is indicative for water signal. Each of the sections shows the water distribution in phase II and III tobacco seeds and each section corresponds to a time window presented in Figure 2A as gray box. The time window, medium (Control or ABA, see Fig. 2), and seed stage are indicated for each section. Each of the sections shows 2D slices from the full 3D NMR microimages as serial sections through three single seeds (one per row) at the given stage. Top two rows of each section, The serial microimages correspond to longitudinal sections with the orientation; radicle at the bottom, shoot at the top (as in drawing I). Bottom row of each section, The serial microimages correspond more or less to transverse sections (as in drawing H). Small white arrows in D indicate the emerged root tip. F and G, Enlarged view of selected NMR microimages in the testa rupture stage (F) and the endosperm rupture stage (G) corresponding to slices presented in C and D, respectively. The small numbers designate the corresponding slices. Left side of each section, Microphotographs of seeds in the testa rupture (F) and endosperm rupture (G) stage. H and I, Drawings of a transverse (H) and a longitudinal (I) section through a germinating tobacco seed are from from Avery (1933).

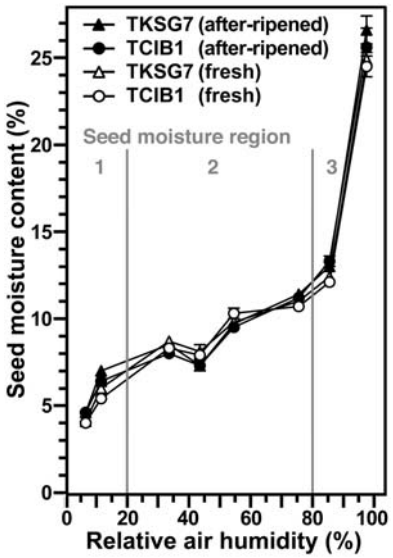

Figure 5. Moisture sorption isotherms of fresh and after-ripened TKSG7 and TCIB1 tobacco seeds. Seeds were incubated for 2 weeks at 24°C above defined saturated salt solutions (Winston and Bates, 1960). Saturated solutions of NaOH, LiCl, $MgCl_2$, K_2CO3, $Mg(NO_3)_2$, NaCl, KCl, and K_2SO4 were used to generate 6%, 11%, 33%, 43%, 54%, 75%, 85%, and 97% relative air humidity, respectively. Seed moisture content is expressed as percentage (w/w) water per FW. Three regions of water availability (1, 2, and 3) can be distinguished and are described in the text. Note that the moisture sorption isotherm of wild-type tobacco seeds (data not shown) did not differ from the presented curves. Mean ±SE of at least five samples are presented for each time point. When error bars are not shown, the ± SE values are <0.5.

not differ between TKSG7 (Fig. 7A; Supplemental Fig. 1, A and C), TCIB1 (Fig. 7, D–F; Supplemental Fig. 1, B and D), and wild type (Fig. 3, B, C, and E). The micropylar endosperm and the radicle of ABA-treated seeds were the tissues with the highest water content (Fig. 7; Supplemental Fig. 1). TKSG7 seeds germinated between 160 and 180 h. The completion of germination was connected with the transition to phase III water uptake, whereas TCIB1 seeds remained in phase II (Figs. 6 and 7B, C, E, and F). During endosperm rupture of TKSG7 (Fig. 7, B and C) and wild-type (Fig. 3, D and G) seeds, the micropylar endosperm and the radicle were the tissues with the highest water contents. Thus, βGlu I overexpression in the covering layers altered the temporal pattern of water uptake but did not affect the spatial distribution of water before and after endosperm rupture.

DISCUSSION

Inhomogeneous Water Distribution during Tobacco Seed Germination: The Micropylar Endosperm and the Radicle Are Major Entry Points of Phase II and III Water Uptake

NMR microimaging showed that water distribution in phase II and III tobacco seeds is inhomogeneous. The micropylar seed end appears to be the major entry point of water. The micropylar endosperm and the radicle show the highest hydration. This spatial pattern of water uptake is already evident during the early phase of imbibition before visible testa rupture. It becomes even more pronounced during testa rupture and remains pronounced after endosperm rupture. Initially, we detected this pattern of water uptake for wild-type tobacco seeds. Further support for it comes from detecting the identical temporal and spatial pattern of water uptake in transgenic TCIB1 tobacco seeds (which have wild-type phenotype). This strongly suggests that the radicle and the micropylar endosperm have enhanced water-holding capacities and can serve as a water reservoir for the embryo during tobacco seed germination.

Our results demonstrate that MRM can be used to analyze the water distribution in imbibed seeds as small as tobacco. Redistribution of water and tissue-specific differences in moisture content has so far

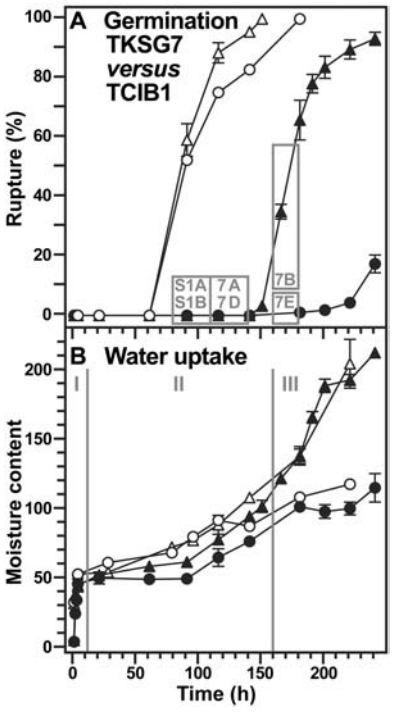

Figure 6. Time course analyses of the effect of βGlu I overexpression on the water uptake during tobacco seed germination in medium with 10 μM ABA. TKSG7 (△, ▲; βGlu I overexpression in seed-covering layers) seeds were compared to TCIB1 (○, ●; empty-vector control, wild-type phenotype with regard to βGlu I and germination) seeds. A, The incidence of testa rupture (white symbols) and endosperm rupture (black symbols). The gray boxes and their numbers correspond to the sections of Figure 7 and Supplemental Figure 1 (S1) showing in vivo NMR microimaging of seeds from these time windows. B, Water uptake measured gravimetrically (black symbols; micrograms water per seed) and by in vivo ^{1}H-MAS NMR (white symbols; relative values). I, II, and III are the three phases of water uptake as described in the text. Mean ± SE of at least three samples are presented for each time point. When error bars are not shown, the ±SE values are <2 (A) or <1 (B).

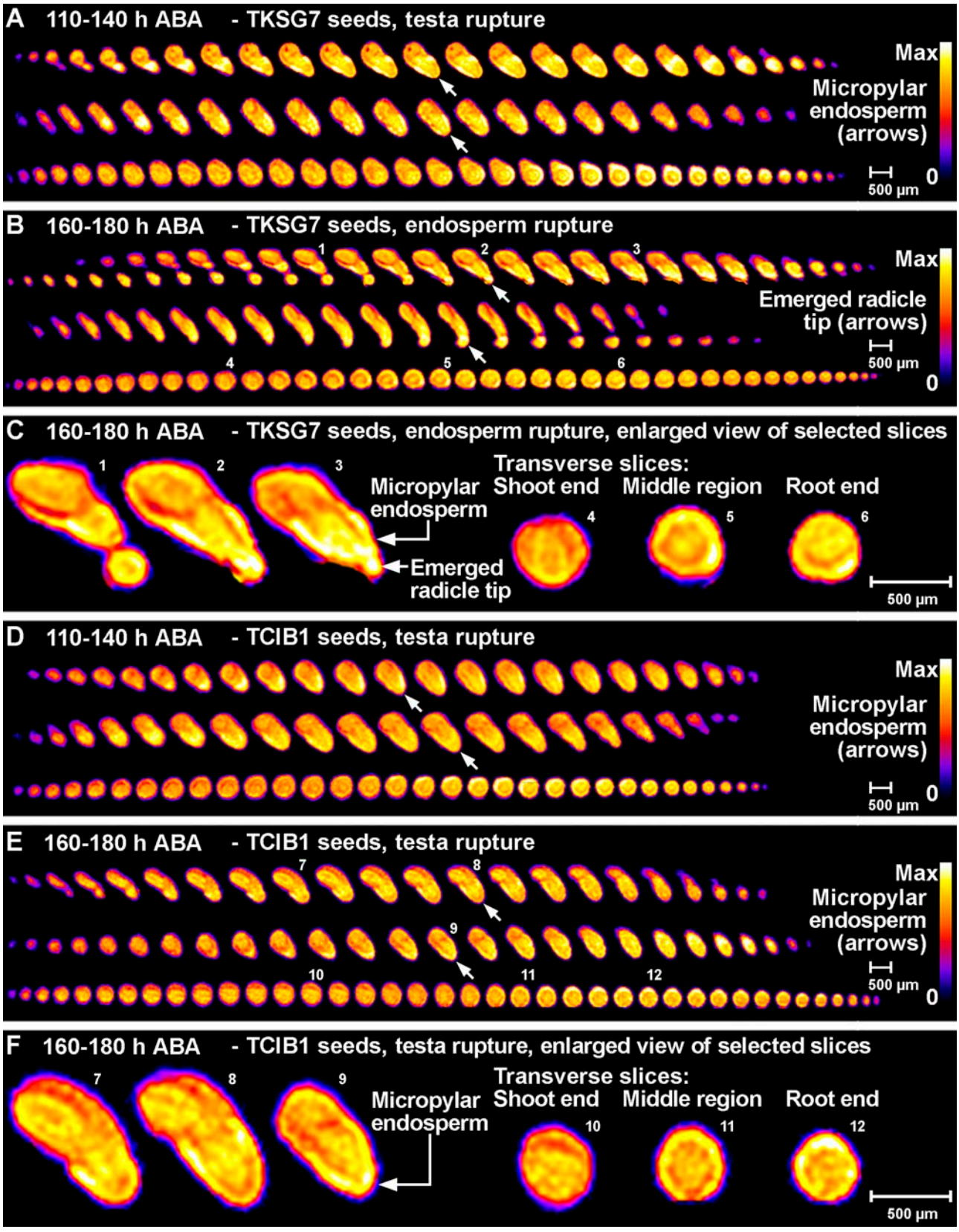

Figure 7. Noninvasive in vivo MRM microimaging analyses of the effect of βGlu I overexpression on water uptake and distribution during tobacco seed germination in medium with 10 µM ABA. The spatial distribution of water within the seed tissues is visualized by false colors (relative scales from zero [0, black] to maximum signal strength [max, white]). A scale bar is given as

been detected only by MRI and MRM of relatively large seeds of trees, legumes, and cereal grains. In developing spruce seeds (*Picea abies*) water was concentrated at the radicle pole (Carrier et al., 1999). In germinating pine seeds (*Pinus monticola*), imbibition is characterized by water penetration through the seed coat and megagametophyte (Terskikh et al., 2005). The cotyledons of the embryo (located in the chalazal end of the seed) are the first to show hydration followed by the hypocotyl and later the radicle. After penetrating the seed coat, water in the micropylar end of the seed likely also contributed to further hydration of the embryo; however, the micropyle itself did not appear to be a site for water entry into the seed (Terskikh et al., 2005). In contrast to pine seeds, the micropylar end of tobacco seeds is the major site for water entry. The micropylar endosperm and the radicle are the first to show hydration followed later by the cotyledons. Thus, these representatives of gymnosperm and angiosperm seeds seem to differ significantly with regard to imbibition. As in tobacco, in bean seeds (*Phaseolus vulgaris*) ethylene-induced germination was associated by ethylene-induced water accumulation at the radicle tip region (Fountain et al., 1998). In tobacco, tomato (*Lycopersicon esculentum*), lettuce, legumes, and other species the seed-covering layers have high contents of galactomannan-type hemicelluloses (Bewley, 1997a; Reid et al., 2003). In legumes, hemicelluloses are known to function as water reservoirs during seed germination and are commercially used as gelling agents (Cunningham and Walsh, 2002). Contrary to bean seeds, tobacco seeds are endospermic. Water uptake has not been investigated by MRM in another endospermic Eudicot seed so far.

The endosperm is a prominent structure in cereal caryopses, but its anatomy differs significantly from tobacco. Differences are also evident in the spatial pattern of water uptake. In imbibed cereal grains, the seed coat and the embryo scutellum region appear to be barriers to water uptake by the embryo (Hou et al., 1997; Gruwel et al., 2002; Krishnan et al., 2004). Prior to germination, water must accumulate in the embryo-scutellum tissues for redistribution to the endosperm to take place. Delayed or protracted hydration severely limits germination. Dissection studies of cereal seeds showed that the hydration properties of seed tissues differ and that the endosperm can act as water reservoir under water-limiting conditions (Stiles, 1948; Hegarty, 1978; Allen et al., 2000). Our results strongly suggest that the micropylar endosperm of tobacco also has such a water reservoir function, but it is already evident under optimal water conditions.

Radicle emergence during the germination of endospermic seeds like tobacco depends on endosperm weakening and on embryo expansion, which is a growth process driven by water uptake (Bewley, 1997b; Leubner-Metzger, 2003). DNA synthesis and cell division are not required, and regulation of the embryo growth potential appears to be mainly by changes in cell wall extensibility. A spatial and temporal pattern of seed aquaporins (Maurel et al., 1997) with a higher density or activity in the radicle and the micropylar endosperm could be involved in generating the uneven water distribution in the germinating tobacco seeds. In principle, it is possible to use images of the tobacco seed moisture contents to perform a spatially resolved moisture content versus time analysis. However, with our existing data this is not possible, because the data presented here were acquired as separate experiments. It is inherent in NMR that the signal intensity depends on the setting of each experiment, like tuning of the probe or quality of the radiofrequency pulses. For future studies it could be possible to use a calibration sample in each experiment, which would then enable a more detailed and spatially resolved analysis.

The molecular mechanism(s) of endosperm weakening seem to be complex (Bewley, 1997a; Leubner-Metzger, 2003). There is strong evidence that hydrolytic enzymes can cause cell wall weakening, which is the precondition for water uptake. Reactive oxygen species can also cause cell wall weakening and are proposed to be involved in shoot and root extension growth, embryo elongation, and endosperm weakening (Schopfer et al., 2001; Leubner-Metzger, 2003). Transcriptional induction of βGlu I genes in the micropylar endosperm in association with endosperm rupture is a widespread phenomenon of Solanaceous seeds (Leubner-Metzger, 2003; Petruzzelli et al., 2003). Sense transformation of tobacco with a chimeric ABA-inducible βGlu I transgene provided direct evidence that βGlu I contributes to endosperm rupture. Whether ABA and βGlu I affect the water uptake needed for embryo expansion and endosperm rupture was therefore a focus of this study.

Figure 7. (*Continued.*)
a size marker. The NMR microimages were obtained with approximately 30 μm resolution. A, B, D, and E, Each of the sections shows 2D slices from full 3D NMR microimages as serial sections through three single seeds (one per row) at the given stage that corresponds to a time window presented in Figure 6A as gray box (110–140 h and 160–180 h, as indicated). Top two rows of each section: The serial microimages correspond to longitudinal sections with the orientation; radicle at the bottom, shoot at the top. Bottom row of each section: The serial microimages correspond more or less to transverse sections. A to C, TKSG7 (βGlu I overexpressing) seeds. D to F, TCIB1 (empty-vector control) seeds. Small white arrows indicate the micropylar endosperm (A, D, and E) or the emerged root tip (B). C and F, Enlarged view of selected NMR microimages of TKSG7 (C) and TCIB1 (F) corresponding to slices presented in B and E, respectively. The small numbers designate the corresponding slices. Note: Corresponding 80 to 110 h results are presented in Supplemental Figure 1.

The inhibition by ABA of tobacco endosperm rupture and phase III water uptake was not due to a spatial effect of ABA on the seed water distribution. Also in ABA-imbibed tobacco seeds, the micropylar endosperm and the radicle were the tissues with the highest (phase II) water content. Testa rupture and initial embryo elongation caused an additional increase in water uptake in the second half of phase II. This additional increase in water content in the late phase II of water uptake seems to be a special feature of endospermic Eudicot seeds with separate testa and endosperm rupture. The additional increase in water content in the late phase II of water uptake is also evident in ABA-treated seeds, which is in agreement with the finding that initial embryo elongation and water uptake by the micropylar endosperm are not inhibited by ABA (e.g. Schopfer and Plachy, 1984; Leubner-Metzger et al., 1995; Homrichhausen et al., 2003). This finding is further supported by water uptake results from dormant tobacco seeds (Mohapatra and Johnson, 1978). Germination of these seeds is blocked before testa rupture, and there is no additional increase in water content in the late phase II of water uptake. ABA therefore inhibits germination and phase III of water uptake by the emerging embryo, but it does not inhibit phase II water uptake needed for initial embryo elongation, and it does not act inhibitory by reducing the water-holding capacity of the micropylar endosperm.

Tobacco Seed Water Status: Low Hydration (Air Moisture Uptake) and Imbibition (Phase I Water Uptake)

Tobacco seeds are oilseeds and dry seeds of the Havana-425 cultivar contain approximately 43% TAGs (seed oil). This is also evident from the typical oilseed moisture sorption isotherm curve. The transition from region 1 (strongly bound water, monolayer) to region 2 (weakly bound water, layers, limited availability) is associated with approximately 7% overall seed moisture content. The transition from region 2 to region 3 (free water, free availability) is associated with approximately 12% overall seed moisture content. In the moisture sorption isotherms for tobacco and other oilseeds, approximately 12% overall moisture content marks the transition to the steep part of the curve, which corresponds to freely available water (Chapman and Robertson, 1987; Multon, 1988; Vertucci, 1989; Mazza and Jayas, 1991; Hay et al., 2003). Seed moisture is absorbed almost exclusively by the carbohydrates and proteins, but not the TAGs. The TAGs are stored in the oil (lipid) bodies of the embryo and the endosperm, and constitute approximately 43% of the seed mass. An overall seed moisture content of 7% (transition region 1–2) and 12% (transition region 2–3) therefore correspond to 12% and 21% overall moisture content in the nonoil seed regions, respectively. In addition, in our earlier work (Leubner-Metzger, 2005), we showed by NMR microimaging that the proton distribution in low-hydrated tobacco seeds is inhomogeneous and that there are areas of high proton content in the outer seed-covering layers. At the higher seed moisture contents during seed imbibition, the proton NMR signals essentially become indicative of water signal. By NMR microimaging, we detected inhomogeneous water distribution and areas with higher water content in the endosperm during early imbibition. These areas might correspond to water-absorbing hemicelluloses in the seed-covering layers (Bewley, 1997a; Cunningham and Walsh, 2002; Reid et al., 2003). Taken together, these findings provide additional support for our earlier proposal of local areas with higher moisture content in the covering layers of low-hydrated tobacco seeds during after-ripening. Thus, the existence of areas with elevated local moisture content and free water is possible in the covering layers of low-hydrated tobacco seeds and permits biochemical reactions and local gene expression during after-ripening (Bove et al., 2005; Leubner-Metzger, 2005). In agreement with our findings for tobacco, the seed-covering layers of many oilseeds are known to have higher water uptake capacities compared to the embryos, e.g. the equilibrium moisture content of the cotton (*Gossypium hirsutum*) or sunflower (*Helianthus annuus*) seed-covering layers is approximately 4% higher compared to the embryos (Karon, 1947; Shatadal and Jayas, 1990; Mazza and Jayas, 1991; American Society of Agricultural Engineers, 2001).

ABA Does Not Inhibit Tobacco Seed Oil Mobilization

By using nondestructive in vivo ^{13}C-MAS NMR spectroscopy, we found that C18:2 is the major fatty acid in tobacco seeds. It is approximately 3-fold as abundant as the second most abundant fatty acids, C18:1Δ9 and C16:0. These results are qualitatively and quantitatively in full agreement with the results obtained by gas chromatography for seeds of other tobacco cultivars (Bush and Grunwald, 1972; Frega et al., 1991). Classical liquid-phase NMR and in vivo ^{13}C-MAS NMR spectroscopy were used in parallel to analyze the TAG and fatty acid contents of lettuce seeds (Bardet et al., 2001). This publication demonstrated that both NMR methods generated the same results and a clear peak assignment was obtained. The comparison of the in vivo ^{13}C-MAS NMR spectra of tobacco and lettuce seeds showed that they are highly similar. Thus, not only is the composition of tobacco and lettuce seed oil highly similar, we could also use the peak assignment for the ^{13}C-MAS NMR spectroscopy to quantify oil mobilization in tobacco seeds.

The total TAG contents and the contents of the single fatty acids C18:2, C18:1Δ9, and C16:0 decreased slightly prior to testa rupture and remained constant during testa and endosperm rupture of tobacco seeds imbibed in control medium. This temporal pattern is in agreement with published results obtained for other tobacco cultivars (Bush and Grunwald, 1972) and for Arabidopsis (Eastmond et al., 2000; Pritchard et al., 2002; Penfield et al., 2004). Mobilization of storage

lipids is mainly a postgermination event and occurs in emerged seedlings. However, as in tobacco and Arabidopsis, an early onset, i.e. prior to the completion of germination, of lipid mobilization was found for castor bean (*Ricinus communis*) endosperm (Marriott and Northcote, 1975), rapeseed (*Brassica napus*) and mustard (*Sinapis alba*) cotyledons (Bergfeld et al., 1978; Hoppe and Theimer, 1997), and sunflower seeds (Fernandez-Moya et al., 2000). In contrast to tobacco and Arabidopsis, a continuous rapid decline in lipid content was observed in these species. Postgermination TAG mobilization in seedlings of several species and TAG mobilization in Arabidopsis embryos is inhibited by ABA (Eastmond et al., 2000; Pritchard et al., 2002; Penfield et al., 2004). In contrast, ABA did not inhibit TAG mobilization in Arabidopsis endosperms (Pritchard et al., 2002; Penfield et al., 2004) and in tobacco seeds (this work). In the mature seeds of these species, the embryo is surrounded by the endosperm, which consists of only a single cell layer in Arabidopsis, but of several cell layers in tobacco. The obvious interpretation of the finding is that, as in Arabidopsis, at least the TAG mobilization in the tobacco endosperm is ABA independent. Taken together, we can conclude from these results that ABA does not inhibit endosperm rupture and transition to postgermination growth by affecting TAG mobilization.

Overexpression of βGlu I Partially Reverts the ABA Inhibition of Endosperm Rupture and Phase III Water Uptake, But Does Not Affect the Water-Holding Capacity

Compared to freshly harvested seeds, after-ripened tobacco seeds have lower ABA contents, decreased ABA sensitivity, and enhanced βGlu I expression during imbibition (Grappin et al., 2000; Leubner-Metzger and Meins, 2000; Leubner-Metzger, 2002, 2005). ABA-sensitive expression of βGlu I in the micropylar endosperm causally contributes to endosperm rupture. This has been directly demonstrated by transgenic TKSG7 tobacco seeds that overexpress βGlu I in the seed-covering layers under the control of an ABA-inducible βGlu I transgene promoter. Neither βGlu I overexpression nor after-ripening altered the seed moisture sorption isotherms. They were identical for freshly harvested and for after-ripened seeds and for TKSG7, TCIB1, and wild-type seeds. In contrast, βGlu I overexpression in the covering layers partially reverted the inhibition by ABA of endosperm rupture and of phase III water uptake. The temporal pattern, but not the spatial pattern, of water uptake was altered in TKSG7 seeds. As for wild type and TCIB1, the micropylar endosperm and the radicle of TKSG7 seeds were the tissues with highest water content. Thus, βGlu I overexpression in the covering layers altered the temporal pattern of water uptake but did not affect the spatial distribution of water before and after endosperm rupture. Taken together, we can conclude from these results that ABA does not inhibit endosperm rupture and transition to postgermination growth by directly affecting the water-holding capacity of the endosperm.

CONCLUSION

Tobacco provides an important model system for endospermic oilseeds. We used the advantage that testa rupture and endosperm rupture are distinct events during tobacco seed germination to assign the triphasic water uptake phases to these events. ABA did not affect testa rupture, initial embryo expansion, and phase I and II water uptake. Testa rupture and initial embryo elongation were associated with an additional phase II increase in water content, which was not inhibited by ABA. ABA inhibited phase III water uptake, endosperm rupture, and the transition to postgermination growth. Overexpression of βGlu I in the seed-covering layers of transgenic tobacco seeds (TKSG7) did not alter the moisture sorption isotherms but partially reverts the ABA inhibition of phase III water uptake and of endosperm rupture. We showed in our studies that in vivo ^{1}H-MAS NMR spectroscopy and MRM are nondestructive methods that can be used to investigate the temporal and spatial pattern of water uptake by seeds as small as tobacco, i.e. <1 mm. They are powerful state-of-the-art technologies that can be used in basic seed research as well as to solve research tasks for the seed industry. We conclude from our in vivo NMR microimaging experiments that the water distribution in the water uptake phases II and III of tobacco seeds is inhomogeneous. The micropylar end of the tobacco seed is not only the place where the testa ruptures and the radicle emerges through the endosperm rupture, it is also the major entry point for water. The micropylar endosperm and the radicle show the highest hydration among the different seed tissues. In vivo ^{13}C-MAS NMR spectroscopy showed that seed oil mobilization is not inhibited by ABA. We conclude from these findings that ABA does not inhibit germination by preventing oil mobilization or by decreasing the water-holding capacity of the micropylar endosperm and the radicle. Our results support the proposal that different seed tissues and organs hydrate at different extents and that the micropylar endosperm region of tobacco acts as a water reservoir for the embryo.

MATERIALS AND METHODS

Plant Materials and Germination Conditions

Seeds of wild-type or transgenic tobacco (*Nicotiana tabacum*) L. cv Havana 425 were harvested at approximately DAP 40 (fresh seeds) and stored for after-ripening for approximately 1 year as described (Leubner-Metzger, 2005). After-ripened seeds were used for all experiments, except for the results presented in Figure 4, where the seed status is indicated. Germination analyses were performed as described earlier (Leubner-Metzger et al., 1995). In brief, approximately 100 seeds were sown in 9-cm-diameter plastic petri

dishes containing filter paper wetted with a nutrient solution and incubated at 24°C (19°C for the experiments presented in Figs. 5 and 6) in continuous white light. Triplicate plates for each time point were used for scoring testa and endosperm rupture. The chimeric-sense βGlu I transgenes of the TKSG7 lines are regulated by the ABA-inducible *Cat1* promoter and TCIB1 (empty vector) lines are the proper controls (Leubner-Metzger and Meins, 2000; Leubner-Metzger, 2002, 2005). The homozygous, monogenic lines TCIB1-2, TKSG7-32, TKSG7-38, and TKSG7-43 were used for this study. The TKSG7 lines have identical germination responses and therefore mean values of the three TKSG7 lines are presented.

Seed Moisture Analyses

Moisture sorption isotherms were obtained by incubating the seeds for 2 weeks at 24°C at defined relative air humidities. These were obtained in sealed vessels above saturated solutions of different salts (Winston and Bates, 1960). The different relative air humidities caused specific equilibrium seed moisture contents (Fig. 4). Saturated solutions of NaOH, LiCl, $MgCl_2$, K_2CO3, $Mg(NO_3)_2$, NaCl, KCl, and K_2SO4 were used to generate 6%, 11%, 33%, 43%, 54%, 75%, 85%, and 97% relative air humidity, respectively. For gravimetric determination of seed moisture contents, the samples were weighed before and after heating for 3 h at 100°C, as described earlier (Leubner-Metzger, 2005). Seed moisture content is expressed as percentage (w/w) water per FW. For the in vivo ^{1}H-MAS NMR spectroscopic analysis of seed moisture, the peak areas below the water signals at 4.8 ppm (Fig. 1A) were quantified.

MAS NMR Spectroscopy and MRM

All NMR experiments were carried out at the Fraunhofer-Institute of Biomedical Engineering, St. Ingbert, Germany (http://www.nmr.fraunhofer.de/) using a Bruker Avance 400 NMR spectrometer (Bruker, Rheinstetten, Germany) with a vertical 9.4 T magnet and a proton resonance frequency of 400 MHz (Manz et al., 2003; Schneider et al., 2003). For MAS NMR spectroscopy, the intact seeds were placed inside a standard 4-mm o.d. MAS rotor. The rotation rate was set to 10 kHz, which has no influence on the seed morphology because, due to the small rotor diameter, the centrifugal forces are low.

For microimaging, the seeds were placed inside a 1.5-mm i.d. glass capillary and, in order to avoid movement during the experiment, pressed slightly against each other with a piece of matching Teflon tube at each end of the glass tube. This capillary was then positioned inside the superconducting magnet (Jenner et al., 1988; Fountain et al., 1998; Manz et al., 2003; Schneider et al., 2003). There is no external movement of the sample tube, e.g. like slow-speed spinning used in high-resolution NMR spectroscopy. The images of the proton density were acquired using a standard Micro2.5 microimaging set and a standard 3D spin-echo pulse sequence (echo time = 1 ms, repetition time = 0.8 s, spectral width 100 kHz) with an isotropical spatial resolution of 30 μm. Each image consisted of 128 × 64 × 64 data points, and two signal averages were taken. The total acquisition time was 110 min per image. ImageJ, the public domain NIH Image program (developed at the United States National Institutes of Health and available on the Internet at http://rsb.info.nih.gov/ij/) was used to obtain the false-colored image slices from the raw data.

^{13}C-MAS NMR Spectroscopic and Biochemical TAG Analyses

Biochemical analysis of TAGs was performed as described by Bergfeld et al. (1978). Batches of approximately 100 seeds were ground with mortar and pestle in 1.5 mL 50% ethanol. Lipids were extracted by vigorous shaking of the homogenate after addition of 500 μL chloroform. An aliquot of 50 μL of chloroform phase was removed and TGAs were hydrolyzed with 500 μL 0.5 M KOH in ethanol. After 10 min, fatty acids were precipitated with 1 mL 150 mM $MgSO_4$ solution. The amount of glycerol was determined in a 450 μL aliquot of the supernatant by a coupled-enzymatic assay at 340 nm (glycerate kinase/pyruvate kinase/lactate dehydrogenase; Bergfeld et al., 1978). Olive oil was used for the calibration curve. For each time point three independent samples were measured. ^{13}C-MAS NMR spectroscopic in vivo analysis of TGAs and fatty acids was performed by quantification of the peak intensities using the appropriate ^{13}C-MAS NMR peak assignments (Pampel et al., 1998; Bardet et al., 2001). TAGs were quantified by measuring the heights of the glycerol peaks (d and e in Fig. 1B), and the fatty acids were quantified by measuring the heights of the appropriate peaks (c, h, and l for C18:2; f and g for C18:1Δ9; Fig. 1B).

ACKNOWLEDGMENTS

We thank Christoph Klüppel, Katrin Hermann, and Barbara Heß for expert technical assistance, and Anja Krieger-Liszkay for critical reading of the manuscript. Research Web site: The Seed Biology Place, http://www.seedbiology.de.

Received February 21, 2005; revised April 14, 2005; accepted April 20, 2005; published June 24, 2005.

LITERATURE CITED

Allen PS, Thorne ET, Gardner JS, White DB (2000) Is the barley endosperm a water reservoir for the embryo when germinating seeds are dried? Int J Plant Sci **161:** 195–201

American Society of Agricultural Engineers (2001) Moisture relationships of plant-based agricultural products. ASAE Standards **D245.5:** 522–538

Avery GSJ (1933) Structure and germination of tobacco seed and the developmental anatomy of the seedling plant. Am J Bot **20:** 309–327

Bardet M, Foray MF (2003) Discrimination of ^{13}C NMR signals in solid material with liquid-like behavior presenting residual dipolar proton-proton homonuclear interactions: application on seeds. J Magn Reson **160:** 157–160

Bardet M, Foray MF, Bourguignon J, Krajewski P (2001) Investigation of seeds with high-resolution solid-state ^{13}C NMR. Magn Reson Chem **39:** 733–738

Bergfeld R, Hong Y-N, Kühnl T, Schopfer P (1978) Formation of oleosomes (storage lipid bodies) during embryogenesis and their breakdown during seedling development in cotyledons of *Sinapis alba* L. Planta **143:** 297–307

Bewley JD (1997a) Breaking down the walls: a role for endo-β-mannanase in release from seed dormancy? Trends Plant Sci **2:** 464–469

Bewley JD (1997b) Seed germination and dormancy. Plant Cell **9:** 1055–1066

Bove J, Lucas P, Godin B, Ogé L, Jullien M, Grappin P (2005) Gene expression analysis by cDNA-AFLP highlights a set of new signaling networks and translational control during seed dormancy breaking in *Nicotiana plumbaginifolia*. Plant Mol Biol **57:** 593–612

Bush PB, Grunwald C (1972) Sterol changes during germination of *Nicotiana tabacum* seeds. Plant Physiol **50:** 69–72

Callaghan PT (1991) Principles of Nuclear Magnetic Resonance Microscopy. Clarendon Press, Oxford

Carrier DJ, Kendall EJ, Bock CA, Cunningham JE, Dunstan DI (1999) Water content, lipid deposition, and (+)-abscisic acid content in developing white spruce seeds. J Exp Bot **50:** 1359–1364

Chapman GW Jr, Robertson JA (1987) Moisture content/relative humidity equilibrium of high-oil and confectionery type sunflower seed. J Stored Prod Res **23:** 115–118

Chudek JA, Hunter G (1997) Magnetic resonance imaging of plants. Prog Nucl Magn Reson Spectrosc **31:** 43–62

Cunningham DC, Walsh KB (2002) Galactomannan content and composition in *Cassia brewsteri* seed. Aust J Exp Agric **42:** 1081–1086

Eastmond PJ, Germain V, Lange PR, Bryce JH, Smith SM, Graham IA (2000) Postgerminative growth and lipid catabolism in oilseeds lacking the glyoxylate cycle. Proc Natl Acad Sci USA **97:** 5669–5674

Eidmann G, Savelsberg R, Blümler P, Blümich B (1996) The NMR MOUSE, a Mobile Universal Surface Explorer. J Magn Reson A **122:** 104–109

Fernandez-Moya V, Martinez-Force E, Garces R (2000) Metabolism of triacyl glycerol species during seed germination in fatty acid sunflower (*Helianthus annuus*) mutants. J Agr Food Chem **48:** 770–774

Finkelstein RR, Lynch TJ (2000) The Arabidopsis abscisic acid response gene *ABI5* encodes a basic leucine zipper transcription factor. Plant Cell **12:** 599–609

Fountain DW, Forde LC, Smith EE, Owens KR, Bailey DG, Callaghan PT

(1998) Seed development in *Phaseolus vulgaris* L. cv. Seminole: NMR imaging of embryos during ethylene-induced precocious germination. Seed Sci Res **8:** 357–365

Frega N, Bocci F, Conte LS, Testa F (1991) Chemical composition of tobacco seeds (*Nicotiana tabacum* L.). J Am Oil Chem Soc **68:** 29–33

Grappin P, Bouinot D, Sotta B, Miginiac E, Jullien M (2000) Control of seed dormancy in *Nicotiana plumbaginifolia*: post-imbibition abscisic acid synthesis imposes dormancy maintenance. Planta **210:** 279–285

Gruwel MLH, Yin XS, Edney MJ, Schroeder SW, MacGregor AW, Abrams S (2002) Barley viability during storage: use of magnetic resonance as a potential tool to study viability loss. J Agr Food Chem **50:** 667–676

Hay FR, Mead A, Manger K, Wilson FJ (2003) One-step analysis of seed storage data and the longevity of *Arabidopsis thaliana* seeds. J Exp Bot **54:** 993–1011

Hegarty TW (1978) The physiology of seed hydration and dehydration, and the relation between water stress and the control of germination: a review. Plant Cell Environ **1:** 101–119

Homrichhausen TM, Hewitt JR, Nonogaki H (2003) Endo-β-mannanase activity is associated with the completion of embryogenesis in imbibed carrot (*Daucus carota* L.) seeds. Seed Sci Res **13:** 219–227

Hoppe A, Theimer RR (1997) Degradation of oil bodies isolated from cotyledons during germination of rapeseed seedlings. J Plant Physiol **151:** 471–478

Hou JQ, Kendall EJ, Simpson GM (1997) Water uptake and distribution in non-dormant and dormant wild oat (Avena fatua L) caryopses. J Exp Bot **48:** 683–692

Jenner CF, Xia Y, Eccles CD, Callaghan PT (1988) Circulation of water within wheat grain revealed by nuclear magnetic resonance micro-imaging. Nature **336:** 399–402

Kamenetsky R, Zemah H, Ranwala AP, Vergeldt F, Ranwala NK, Miller WB, van As H, Bendel P (2003) Water status and carbohydrate pools in tulip bulbs during dormancy release. New Phytol **158:** 109–118

Karon ML (1947) Hygroscopic equilibrium of cottonseed. J Am Oil Chem Soc **24:** 56–59

Köckenberger W, de Panfilis C, Santoro D, Dahiva P, Rawsthorne S (2004) High resolution NMR microscopy of plants and fungi. J Microsc **214:** 182–189

Koornneef M, Bentsink L, Hilhorst H (2002) Seed dormancy and germination. Curr Opin Plant Biol **5:** 33–36

Korb JP, Godefroy S, Fleury M (2003) Surface nuclear magnetic relaxation and dynamics of water and oil in granular packings and rocks. Magn Reson Imaging **21:** 193–199

Krishnan P, Joshi DK, Nagarajan S, Moharir AV (2004) Characterisation of germinating and non-germinating wheat seeds by nuclear magnetic resonance (NMR) spectroscopy. Eur Biophys J **33:** 76–82

Krock B, Schmidt S, Hertweck C, Baldwin IT (2002) Vegetation-derived abscisic acid and four terpenes enforce dormancy in seeds of the post-fire annual, *Nicotiana attenuata*. Seed Sci Res **12:** 239–252

LaTorraca GA, Dunn KJ, Webber PR, Carlson RM (1998) Low-field NMR determinations of the properties of heavy oils and water-in-oil emulsions. Magn Reson Imaging **16:** 659–662

Leubner-Metzger G (2002) Seed after-ripening and over-expression of class I β-1,3-glucanase confer maternal effects on tobacco testa rupture and dormancy release. Planta **215:** 959–968

Leubner-Metzger G (2003) Functions and regulation of β-1,3-glucanase during seed germination, dormancy release and after-ripening. Seed Sci Res **13:** 17–34

Leubner-Metzger G (2005) β-1,3-Glucanase gene expression in low-hydrated seeds as a mechanism for dormancy release during tobacco after-ripening. Plant J **41:** 133–145

Leubner-Metzger G, Fründt C, Vögeli-Lange R, Meins F Jr (1995) Class I β-1,3-glucanase in the endosperm of tobacco during germination. Plant Physiol **109:** 751–759

Leubner-Metzger G, Meins F Jr (2000) Sense transformation reveals a novel role for class I β-1,3-glucanase in tobacco seed germination. Plant J **23:** 215–221

Lopez-Molina L, Mongrand S, Chua N-H (2001) A postgermination developmental arrest checkpoint is mediated by abscisic acid and requires ABI5 transcription factor in *Arabidopsis*. Proc Natl Acad Sci USA **98:** 4782–4787

MacFall JS, van As H (1996) Magnetic resonance imaging of plants. *In* Y Shachar-Hill, PE Pfeffer, eds, Nuclear Magnetic Resonance in Plant Biology, Vol 16. American Society of Plant Biologists, Rockville, MD, pp 33–76

Mansfield P, Morris PG (1982) NMR Imaging in Biomedicine. Academic Press, New York

Manz B, Alexander P, Gladden LF (1999) Correlations between dispersion and structure in porous media probed by NMR. Phys Fluids **11:** 259–267

Manz B, Volke F, Goll D, Horn H (2003) Measuring local flow velocities and biofilm structure in biofilm systems with magnetic resonance imaging (MRI). Biotechnol Bioeng **84:** 424–432

Marriott KM, Northcote DH (1975) The breakdown of lipid reserves in the endosperm of germinating castor beans. Biochem J **148:** 139–144

Maurel C, Chrispeels M, Lurin C, Tacnet F, Geelen D, Ripoche P, Guern J (1997) Function and regulation of seed aquaporins. J Exp Bot **48:** 421–430

Mazza G, Jayas DS (1991) Equilibrium moisture characteristics of sunflower seeds, hulls, and kernels. Trans ASAE **34:** 534–538

Mohapatra SC, Johnson WH (1978) Development of the tobacco seedling: relationship between moisture uptake and light sensitivity during seed germination in a flue-cured variety. Tob Res **4:** 41–49

Multon JL (1988) Interactions between water and the constituents of grains, seeds and by-products. *In* JL Multon, AM Reimbert, D Marsh, AJ Eydt, eds, Preservation and Storage of Grains, Seeds and Their By-Products. Lavoisier Publishing, New York, pp 89–159

Obroucheva NV, Antipova OV (1997) Physiology of the initiation of seed germination. Russ J Plant Physiol **44:** 250–264

Pampel A, Strandberg E, Lindblom G, Volke F (1998) High-resolution NMR on cubic lyotropic liquid crystalline phases. Chem Phys Lett **287:** 468–474

Penfield S, Rylott EL, Gilday AD, Graham S, Larson TR, Graham IA (2004) Reserve mobilization in the Arabidopsis endosperm fuels hypocotyl elongation in the dark, is independent of abscisic acid, and requires PHOSPHOENOLPYRUVATE CARBOXYKINASE1. Plant Cell **16:** 2705–2718

Petruzzelli L, Müller K, Hermann K, Leubner-Metzger G (2003) Distinct expression patterns of β-1,3-glucanases and chitinases during the germination of Solanaceous seeds. Seed Sci Res **13:** 139–153

Pouliquen D, Gross D, Lehmann V, Ducournau S, Demilly D, Lechappe J (1997) Study of water and oil bodies in seeds by nuclear magnetic resonance. C R Acad Sci III **320:** 131–138

Prado PJ (2001) NMR hand-held moisture sensor. Magn Reson Imaging **19:** 505–508

Pritchard SL, Charlton WL, Baker A, Graham IA (2002) Germination and storage reserve mobilization are regulated independently in Arabidopsis. Plant J **31:** 639–647

Ratcliffe RG (1996) In vivo NMR spectroscopy: biochemical and physiological applications to plants. *In* Y Shachar-Hill, PE Pfeffer, eds, Nuclear Magnetic Resonance in Plant Biology, Vol 16. American Society of Plant Biologists, Rockville, MD, pp 1–32

Reid JSG, Edwards ME, Dickson CA, Scott C, Gidley MJ (2003) Tobacco transgenic lines that express fenugreek galactomannan galactosyltransferase constitutively have structurally altered galactomannans in their seed endosperm cell walls. Plant Physiol **131:** 1487–1495

Roh MS, Bentz J-A, Wang P, Li E, Koshioka M (2004) Maturity and temperature stratification affect the germination of *Styrax japonicus* seeds. J Hortic Sci Biotechnol **79:** 645–651

Schmidt SJ (1991) Determination of moisture content by pulsed nuclear magnetic resonance spectroscopy. Adv Exp Med Biol **302:** 599–613

Schneider H, Manz B, Westhoff M, Mimietz S, Szimtenings M, Neuberger T, Faber C, Krohne G, Haase A, Volke F, et al (2003) The impact of lipid distribution, composition and mobility on xylem water refilling of the resurrection plant *Myrothamnus flabellifolia*. New Phytol **159:** 487–505

Schopfer P, Plachy C (1984) Control of seed germination by abscisic acid: effect on embryo water uptake in *Brassica napus* L. Plant Physiol **76:** 155–160

Schopfer P, Plachy C, Frahry G (2001) Release of reactive oxygen intermediates (superoxide radicals, hydrogen peroxide, and hydroxyl radicals) and peroxidase in germinating radish seeds controlled by light, gibberellin, and abscisic acid. Plant Physiol **125:** 1591–1602

Schwachtje J, Baldwin IT (2004) Smoke exposure alters endogenous gibberellin and abscisic acid pools and gibberellin sensitivity while eliciting germination in the post-fire annual, *Nicotiana attenuata*. Seed Sci Res **14:** 51–60

Shatadal P, Jayas DS (1990) Moisture sorption isotherms of grains and oilseeds. Postharvest News Inf **1:** 447–451

Stiles IE (1948) Relation of water to the germination of corn and cotton seeds. Plant Physiol **23:** 201–222

Terskikh VV, Feurtado JA, Ren C, Abrams SR, Kermode AR (2005) Water uptake and oil distribution during imbibition of seeds of western pine (*Pinus monticola* Dougl. ex D. Don) monitored in vivo using magnetic resonance imaging. Planta **221:** 17–27

Vertucci CW (1989) The effects of low water contents on physiological activities of seeds. Physiol Plant **77:** 172–176

Volke F, Pampel A, Haensler M, Ullmann G (1996) Proton MAS NMR of a protein in frozen aqueous solution. Chem Phys Lett **262:** 374–378

Winston PW, Bates DH (1960) Saturated solutions for the control of humidity in biological research. Ecology **41:** 232–237

Wolter B (2001) ^{1}H-NMR-Verfahren in aufsatztechnik zur zerstörungsfreien charakterisierung zementgebundener und organischer poröser Werkstoffe. PhD thesis. Universität des Saarlandes, Saarbrücken, Germany